Neutron-Rich Ti Isotopes And Possible N = 32 And N = 34 Shell Gaps

D.-C. Dinca[*†], R. V. F. Janssens[**], A. Gade[†], B. Fornal[‡], S. Zhu[**], D. Bazin[†], R. Broda[‡], C. M. Campbell[*†], M. P. Carpenter[**], P. Chowdhury[**§], J. M. Cook[*†], P. J. Daly[¶], A. N. Deacon[‖], S. J. Freeman[‖], T. Glasmacher[†], Z. W. Grabowski[¶], N. J. Hammond[**], F. G. Kondev[††], W. Królas[‡], T. Lauritsen[**], J.-L. Lecouey[†], S. N. Liddick[†‡‡], C. J. Lister[**], P. F. Mantica[†‡‡], E. F. Moore[**], W. F. Mueller[†], H. Olliver[*†], T. Pawłat[‡], D. Seweryniak[**], K. Starosta[*†], J. R. Terry[*†], B. E. Tomlin[†‡‡], J. Wrzesiński[‡] and K. Yoneda[†]

[*] *Department of Physics and Astronomy, Michigan State University, East Lansing, MI 48824, USA*
[†] *National Superconducting Cyclotron Laboratory, Michigan State University, East Lansing, MI 48824, USA*
[**] *Physics Division, Argonne National Laboratory, Argonne, IL 60439, USA*
[‡] *Institute of Nuclear Physics, Polish Academy of Sciences, PL-31342 Cracow, Poland*
[§] *University of Massachusetts Lowell, Lowell, MA 01854, USA*
[¶] *Chemistry and Physics Departments, Purdue University, West Lafayette, Indiana 47907*
[‖] *Department of Physics and Astronomy, Schuster Laboratory, University of Manchester, Manchester M13 9PL, United Kingdom*
[††] *Nuclear Engineering Division, Argonne National Laboratory, Argonne, Illinois 60439, USA*
[‡‡] *Department of Chemistry, Michigan State University, East Lansing, MI 48824, USA*

Abstract. The possible occurrence of sub-shell gaps at N = 32 and N = 34 in neutron-rich titanium isotopes is discussed in light of new experimental results from (i) deep-inelastic reactions measured with Gammasphere at the ATLAS facility at Ar gonne National Laboratory and from (ii) intermediate-energy Coulomb excitation performed at the National Superconducting Cyclotron Laboratory at Michigan State University.

INTRODUCTION

Shell structure is the foundation for much of our present understanding of atomic nuclei, although most of our knowledge about the ordering and location in energy of the single-particle states remains empirical. In this context, neutron-rich nuclei have become the focus of recent theoretical and experimental efforts. The on-going investigations are motivated to a large extent by expectations of substantial modifications of shell structure in nuclei with a sizable neutron excess. Shell-model calculations with the full *pf* shell predict that as the number of protons occupying the orbit $\pi f_{7/2}$ decreases, the $\pi f_{7/2}$ - $\nu f_{5/2}$ monopole pairing interaction strength weakens. As a consequence, the orbital $\nu f_{5/2}$ is shifted up in energy. This effect combined with a significant spin-orbit splitting beween the $\nu p_{1/2}$ and $\nu p_{3/2}$ orbitals leads to possible sub-shell gaps at neutron number N = 32 and N = 34. Specifically, calculations with the recently developed GXPF1 effective interaction [1] predict sub-shell gaps for Ca and Ti isotopes at N = 32 and N = 34, and at N = 32 for Cr.

DEEP-INELASTIC STUDIES OF ^{56}TI

The properties of ^{56}Ti have been studied at the ATLAS accelerator with Gammasphere [2] using deep-inelastic reactions induced by a 330 MeV ^{48}Ca beam on a ^{238}U, 50 mg/cm^2-thick target. The trigger condition required three or

CP764, *Nuclei at the Limits,* edited by D. Seweryniak and T. L. Khoo

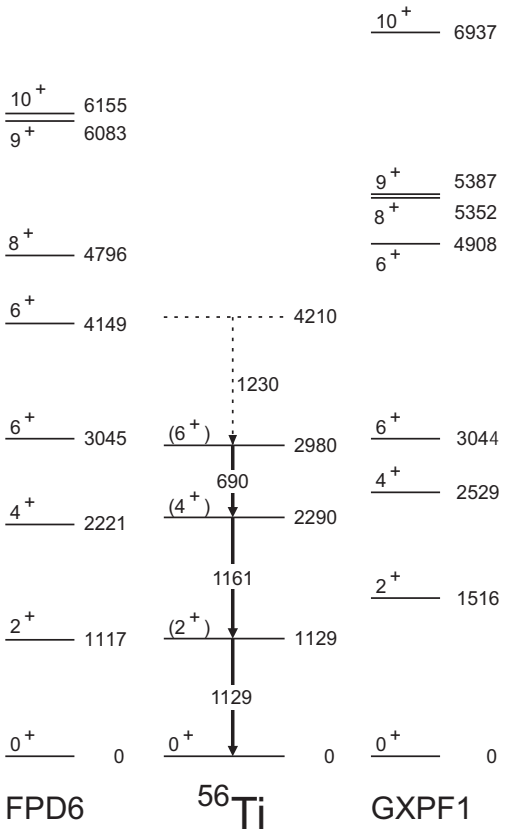

FIGURE 1. Comparison of the ^{56}Ti level scheme deduced from the experimental data (center), and two shell model calculations using the FPD6 (left) and GXPF1 (right) effective interactions.

more Compton-suppressed γ rays in prompt coincidence. The beam was pulsed with an approximate 420 ns period to allow a clean separation between prompt and isomeric decays. In a previous experiment [3], deep inelastic reactions with a ^{48}Ca beam at 305 MeV on a thick ^{208}Pb target had been used to explore the yrast excitations of ^{52}Ti and ^{54}Ti. In order to produce Ti nuclei with larger neutron excess, such as ^{56}Ti, advantage was taken of the larger neutron reservoir provided by ^{238}U. It was found that scattering of a ^{238}U target provides a four-times higher ^{56}Ti yield compared to the ^{208}Pb target, but the characteristics of the reaction process make the data analysis more difficult. The target-like products of deep inelastic collisions mostly undergo fission in this case and an identification based on cross-coincidences between γ rays from both reaction partners is impossible. Because of this, the starting point of the analysis was a 1127 keV γ ray known from previous β-decay measurements [4], identified as the $2^+ \rightarrow 0^+$ transition in ^{56}Ti. A γ ray at 1161 keV was found in coincidence. Then, by using double coincidence relationships, a transition at 690 keV was established. Double gating on different combinations among these three lines confirmed their mutual coincidence relationships. Since deep-inelastic reactions preferentially populate yrast states and because the 4^+ and 6^+ levels in ^{56}Ti are expected to correspond to proton excitations of $\pi f_{7/2}^2$ character with energy spacings $E(4^+\text{-}2^+) > E(6^+\text{-}4^+)$, the 1161 keV transition was assigned as $4^+ \rightarrow 2^+$ and the 690 keV line as $6^+ \rightarrow 4^+$. There is an indication of another γ ray at 1230 keV, a possible $8^+ \rightarrow 6^+$ transition, but spectra with higher statistics are needed to make a firm assignment.

A good agreement with shell-model calculations using the FPD6 effective interaction is observed [Fig. 1]. However, it should be noted that this interaction does not reproduce the experimental data for the titanium isotopes with mass 52 and 54. A significant disagreement between experiment and GXPF1, of about 400 keV, is observed for the first 2^+ state. We return to this point further below.

COULOMB EXCITATION STUDIES OF ^{52,54,56}TI

The presence of sub-shell gaps can be probed further through the measurement of the electromagnetic transition rates to the first excited 2^+ states of the ^{52,54,56}Ti isotopes with the technique of intermediate-energy Coulomb excitation [5]. This study was carried out at the National Superconducting Cyclotron Laboratory with the Segmented Germanium Array (SeGA) [6] in conjunction with the S800 spectrograph [7]. In this method, the collision takes place well above the Coulomb barrier. To avoid nuclear contributions to the electromagnetic process, the impact parameter must be kept large. The impact parameter can be controlled by limiting the scattering angle of the projectiles. [5]

A primary beam of ^{76}Ge extracted from the ion source at charge state 12^+ was first accelerated in the K500 cyclotron to an energy of 11.59 MeV/nucleon, then injected into the K1200 cyclotron after the average charge state was increased to 30^+ using a stripper foil system. After the acceleration, the beam was extracted at an energy of 130 MeV/nucleon and an average intensity of 10 pnA . The fragments were produced by impinging the beam on a 382 mg/cm ^{2}-thick ^{9}Be primary target. The A1900 fragment separator [8] selected the desired isotopes and directed them to the target position of the S800 spectrograph. Four settings were used in the experiment: a test case with the primary beam (^{76}Ge) degraded to 81 MeV/nucleon on a 256 mg/cm^2-thick ^{197}Au target, a ^{52}Ti secondary beam at 89 MeV/nucleon on gold targets with two thicknesses, 256 mg/cm^2 and 518 mg/cm^2, a ^{54}Ti secondary beam (88 MeV/nucleon) on a 256 mg/cm ^{2}-thick ^{197}Au target and a ^{56}Ti secondary beam (88 MeV/nucleon) impinging on a 518 mg/cm ^{2}-thick ^{197}Au target. Fifteen of the total of 18 segmented HPGe detectors of SeGA were used, grouped in two rings around the target [9, 10].

Two scintillators before the target were used for time-of-flight measurements, two Parallel Plate Avalanche Counters (PPAC) allowed for secondary beam tracking, and two Cathode Readout Drift Chambers (CRDC) (1 meter apart) provided the position and angle information in the focal plane of the spectrograph. An ion chamber was used to determine the energy loss of the ions and two plastic scintillators at the very end provided time-of-flight and energy loss information together with trigger signals. The data acquisition system triggered on either one of two conditions, a particle-gamma prompt coincidence or a down-scaled particle. The Lorentz boosted gamma rays are detected in the laboratory frame. To reconstruct the energies in the projectile frame, an event-by-event Doppler correction was applied using the energy recorded by the central contact of the detectors and the information from the segments.

Along with the Coulomb excitation of the beam particles, the excitation of the target nuclei occurs as well. In the data analysis, these two processes share the same kinematics, particle identification and angle cuts, providing a cross check for a large part of the experimental conditions. Calculation of the excitation cross section requires the following values to be known: the number of particles in the beam, the number of gamma rays detected, the gamma-ray detection efficiency, and the number of nuclei in the target. The photopeak efficiency for the array was measured with standard calibration sources at the target position. For moving sources, because of the Lorentz boost and the angular distribution of the emitted gamma rays, the efficiency was simulated with GEANT3 [11]. The accuracy of the simulation was verified by simulating also static sources and comparing the results with the measured values of the efficiency. Figure 2 shows event-by-event Doppler corrected spectra for ^{76}Ge (a), ^{52}Ti (b), ^{54}Ti (c), ^{56}Ti (d). Figure 3 compares the results obtained in the present measurements [12] for Coulomb excitation of the ^{197}Au target with the adopted value from the literature [13]. The good agreement between all these values gives further confidence in the experimental approach.

DISCUSSION

Experimental evidence for a shell closure is usually inferred from at least two observables derived from nuclear spectra: the energy of the first excited state and the reduced transition probability to the same level. Figure 4 presents the two physical quantities of interest for all even Ti isotopes with mass A = 48 to A = 56. From the figure, a clear anti-correlation between the two observables can be readily seen: while the $E(2^+)$ energies increase significantly at N = 28 and N = 32 (Fig. 3(a)), the $B(E2;0^+ \rightarrow 2^+)$ strengths are lowest for these two neutron numbers (Fig. 3(b)). Furthermore, both these physical quantities also differ markedly from the corresponding values at neutron numbers N = 26, 30 and 34. For ^{50}Ti, the well known shell closure at N = 28 translates into a small transition probability and a high 2^+ excitation energy. The fact that the excitation energy and the reduced transition probability observed in ^{54}Ti are comparable to those in ^{50}Ti suggests that the Ti isotope with N = 32 is as good a semi-magic nucleus as its N = 28 counterpart and, hence, that a substantial sub-shell gap must occur at N = 32. Conversely, the fact that the three other Ti isotopes have 2^+ excitation energies lower by several hundreds of keV and $B(E2;0^+ \rightarrow 2^+)$ values higher by a factor of ~ 2 can be interpreted as an experimental indication for the absence of sub-shell gaps in the neutron single-particle

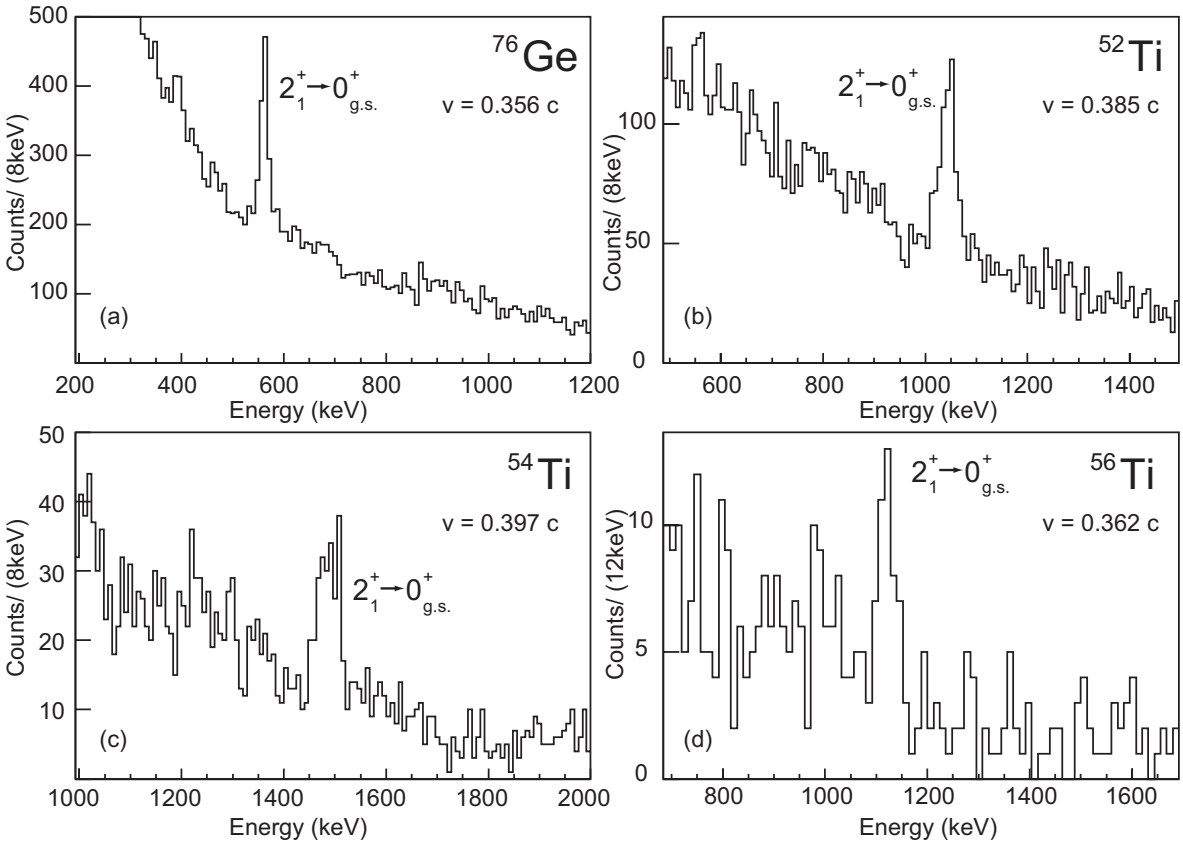

FIGURE 2. Representative spectra for ^{76}Ge and the even $^{52-56}$Ti isotopes in the laboratory frame.

spectrum at N = 26, 30 and 34. The lines in Fig. 4 are the result of shell model calculations with the GXPF1 effective interaction; while the N = 32 gap in the Ti isotopes is accounted for, the calculations also predict an additional gap at N = 34 that is not borne out by experiment. The data suggest instead that the energy spacings between the $p_{3/2}$, $p_{1/2}$ and $f_{5/2}$ neutron orbitals, as well as the degree of admixture between these states in the wavefunctions of the ^{56}Ti yrast excitations, require further theoretical investigation. Such investigations are presently under way.

ACKNOWLEDGMENTS

The authors thank T. Baumann, A. Stolz, T. Ginter and M. Steiner and the NSCL cyclotron operations group for providing the secondary and primary beams required for these measurements. Many thanks also to the ATLAS operation staff for the flawless operation of the accelerator and to the ANL Physics Division technical support group for assistance in the preparation of the experiment. This work is supported in part by National Science Foundation grant Nos. PHY-01-10253, PHY-02-44453, PHY-97-24299, and PHY-98-75122, by the U. S. Department of Energy, Office of Nuclear Physics, under contracts W–31–109–ENG–38, and DE–FG02–94ER40848, by grant No. 2PO3B-074-18 of the Polish Scientific Committee, and by the UK Engineering and Physical Sciences Research Council (EPSRC).

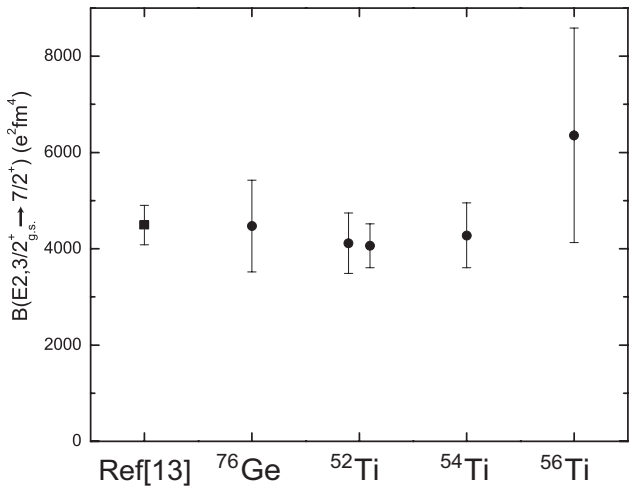

FIGURE 3. Comparison of the $B(E2;3/2^+_{g.s.} \rightarrow 7/2^+)$ adopted value [13] (solid square) for ^{197}Au, with the measured values from the present experiment [12] (solid circles).

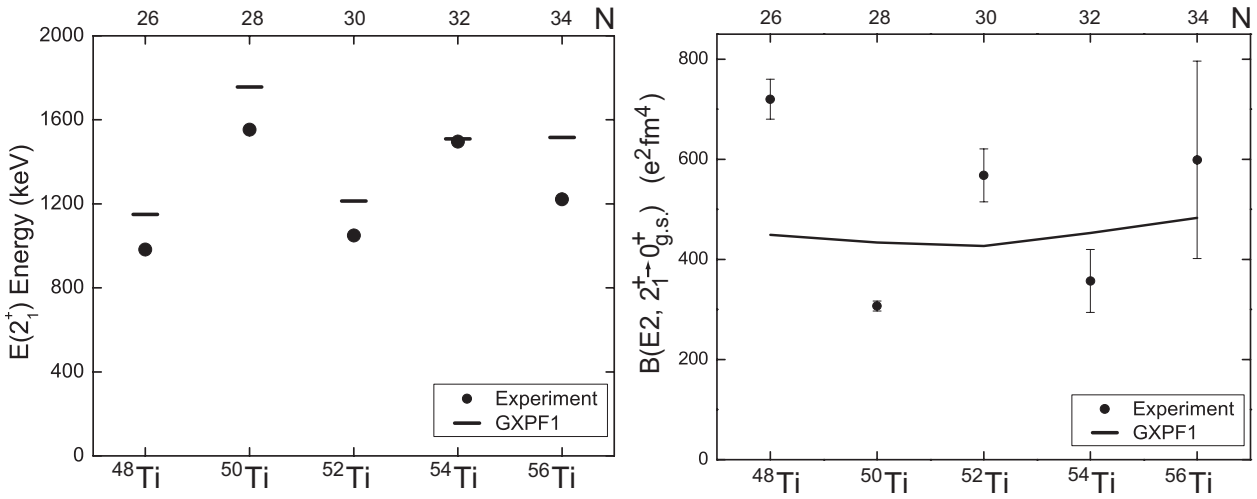

FIGURE 4. Comparison of the 2^+ energies and $B(E2;0^+ \rightarrow 2^+)$ values for $^{48-56}$Ti with the results of shell model calculations with the GXPF1 interaction.

REFERENCES

1. M. Honma *et al.*, Phys. Rev. C **65**, 061301 (2002).
2. I. Y. Lee, Nucl. Phys. **A520**, 641c (1990).
3. R. V. F. Janssens *et al*., Phys. Lett. **B546**, 55 (2002).
4. S. N. Liddick *et al*., Phys. Rev. Lett. **92**, 072502 (2004), and *ibid.* Phys. Rev. C (in press).
5. T. Glasmacher, Annu. Rev. Nucl. Part. Sci. **48**, 1 (1998).
6. W. F. Mueller *et al.*, Nucl. Instrum. Methods Phys. Res. **A466**, 492 (2001).
7. D. Bazin *et al.*, Nucl. Instrum. Methods Phys. Res. **B204**, 629 (2003).
8. D. J. Morrissey *et al.*, Nucl. Instrum. Methods Phys. Res. **B204**, 90 (2003).
9. A. Gade *et al.*, Phys. Rev. C **68**, 014302 (2003).
10. K. L. Yurkewicz *et al.*, Phys. Rev. C **70**, 034301 (2004).
11. GEANT, version 3.21, CERN program library, W5013, 1994.
12. D.-C. Dinca *et al.*, submitted for publication.
13. Zhou Chunmei, Nuclear Data Sheets **76**, 399 (1995).